3D non-LTE corrections for the ^{6}Li/^{7}Li isotopic ratio in solar-type stars

G. Harutyunyan[1,2], M. Steffen[1], A. Mott[1,2], E. Caffau[3], G. Israelian[4],

J.I. González Hernández[4], and K.G. Strassmeier[1]

[1] Leibniz-Institut für Astrophysik Potsdam, An der Sternwarte 16, 14482 Potsdam, Germany,
e-mail: `gharutyunyan@aip.de`

[2] Universität Potsdam, Institut für Physik und Astronomie, Karl-Liebknecht-Straße 24/25,
14476 Potsdam, Germany

[3] GEPI, Observatoire de Paris, PSL Research University, CNRS, Place Jules Janssen, 92190
Meudon, France

[4] Instituto de Astrofsica de Canarias, 38200 La Laguna, Tenerife, Spain

Abstract. Doppler shifts induced by convective motions in stellar atmospheres affect the shape of spectral absorption lines and create slightly asymmetric line profiles. It is important to take this effect into account in modeling the subtle depression created by the ^{6}Li isotope which lies on the red wing of the Li I 670.8 nm resonance doublet line, since convective motions in stellar atmospheres can mimic a presence of ^{6}Li when intrinsically symmetric theoretical line profiles are presumed for the analysis of the ^{7}Li doublet (Cayrel et al. 2007). Based on CO5BOLD hydrodynamical model atmospheres, we compute 3D non-local thermodynamic equilibrium (NLTE) corrections for the ^{6}Li/^{7}Li isotopic ratio by using a grid of 3D NLTE and 1D LTE synthetic spectra. These corrections must be added to the results of the 1D LTE analysis to correct them for the combined 3D non-LTE effects. As one would expect, the resulting corrections are always negative and they range between 0 and -5 %, depending on effective temperature, surface gravity, and metallicity. For each metallicity we derive an analytic expression approximating the 3D NLTE corrections as a function of effective temperature, surface gravity and projected rotational velocity.

Key words. stars: abundances – stars: atmospheres – stars: convection – stars: solar-type – line: profiles

1. Introduction

The lithium abundance and the ^{6}Li/^{7}Li isotopic ratio measured in stars can provide valuable information contributing to different problems in stellar structure and stellar evolution, stellar activity, and even cosmology. A reliable determination of the lithium content of stellar atmospheres requires not only high resolution and high signal-to-noise spectra, but also realistic stellar atmosphere models allowing a good theoretical interpretation of both the strength and the shape of Li lines.

Both stable lithium isotopes (^{6}Li and ^{7}Li) are very fragile with respect to nuclear reac-

tions and are destroyed in stellar interiors at temperatures above $\sim 2.5 \times 10^6$ K ($\sim 2.0 \times 10^6$ K for ^{6}Li) (e.g., Pinsonneault 1997). Current standard stellar evolution models predict an intense destruction of ^{6}Li during the pre-main sequence phase. It is then expected that, by the time a solar-type star reaches the main sequence, its ^{6}Li has already been destroyed by nuclear reactions at the base of the extended, completely mixed convective envelope. Any detection of this fragile isotope in an atmosphere of a solar-type star would most probably indicate an external pollution process, for example by planetary matter accretion (Israelian et al. 2001) or alternative sources like stellar flares (Montes & Ramsey 1998). Therefore, it is of great interest to measure the presence of the ^{6}Li isotope in solar-type stars and, in case of a positive detection, to investigate its origin.

The use of one-dimensional (1D) model atmospheres can lead to erroneous results in terms of lithium isotopic ratios, due to the fact that the missing convective line asymmetry must be compensated by a non-real ^{6}Li abundance to fit the observed line profile. The result is an overestimation of the ^{6}Li/^{7}Li ratio using 1D model atmospheres (e.g. Steffen et al. 2012). Instead, the use of detailed three-dimensional (3D) hydrodynamical model atmospheres allows to obtain more reliable abundances and isotopic ratios in particular, since they are able to treat the convective motions responsible of the line asymmetries in a much more realistic way compared to standard 1D model atmospheres. In addition to this, in the case of lithium, the line formation can be treated considering departures from LTE that are known to be significant especially in metal-poor stars (Cayrel et al. 2007). On the other hand, 3D NLTE calculations are computationally demanding and not easily accessible to the scientific community. For this reason, it is important to employ some simplified approaches to account for both 3D and NLTE effects in studying the lithium line region through spectral synthesis.

In this work, we use a grid of synthetic spectra computed from 3D hydrodynamical CO5BOLD models and 1D hydrostatic LHD model atmospheres for a range of stellar parameters for solar-type stars. The intention is to provide a set of 3D NLTE corrections for the ^{6}Li/^{7}Li ratio that can be directly used to correct the results of 1D LTE analyses.

2. Methods

2.1. Model atmospheres

In this study, we use a small grid of CO5BOLD 3D hydrodynamical model atmospheres (Freytag et al. 2002, 2012) taken from the CIFIST 3D atmosphere grid (Ludwig et al. 2009). The models are computed for combinations of three different effective temperatures (T_{eff}), two different surface gravities ($\log g$), and four different metallicities ([Fe/H]). In total, the grid consists of 24 3D model atmospheres (for details, see Table 1). To each CO5BOLD model in our grid, we associate a 1D LHD model atmosphere (Caffau et al. 2008) having the same effective temperature, metallicity and surface gravity. The advantage of using these particular one-dimensional model atmospheres is that they employ the same opacity tables and equation of state, allowing to minimize possible intrinsic differences in our differential analysis, other than 3D effects. The final T_{eff} of each CO5BOLD hydrodynamical model is determined after a manual selection of a number of representative snapshots (N snaps. in Table 1) and differs slightly from the nominal temperature value. For this reason, the models in our grid do not have exactly the same effective temperatures. The number of opacity bins (N bins) for each model is given in Table 1.

2.2. Linelists

In the present work, we adopt three different list of atomic and molecular lines for synthesizing the Li I 670.8 nm region. The first line list considers only the Li I atomic lines taken from Kurucz (1995); the original table of transitions was simplified to include six ^{6}Li and six ^{7}Li components (hereafter, Linelist 1). The second one was constructed by Ghezzi et al. (2009) and slightly modified by Delgado Mena et al. (2014) (hereafter, Linelist 2) and the

Table 1. CO5BOLD 3D hydrodynamical model atmospheres used in this work.

Model N	T_{eff} [K]	$\log g$	[Fe/H]	N snap.	N bins
1	5850	4.0	−1.0	20	6
2	5920	4.5	−1.0	8	6
3	6260	4.0	−1.0	20	6
4	6240	4.5	−1.0	20	6
5	6500	4.0	−1.0	20	6
6	6500	4.5	−1.0	19	6
7	5920	4.0	−0.5	20	6
8	5900	4.5	−0.5	20	6
9	6250	4.0	−0.5	20	6
10	6230	4.5	−0.5	20	6
11	6500	4.0	−0.5	20	6
12	6500	4.5	−0.5	20	6
13	5930	4.0	0.0	18	5
14	5870	4.5	0.0	19	5
15	6230	4.0	0.0	20	5
16	6230	4.5	0.0	20	5
17	6490	4.0	0.0	20	5
18	6500	4.5	0.0	20	5
19	5870	4.0	0.5	20	5
20	5900	4.5	0.5	20	5
21	6190	4.0	0.5	20	5
22	6350	4.5	0.5	20	5
23	6500	4.0	0.5	20	5
24	6500	4.5	0.5	20	5

third one has been taken from Meléndez et al. (2012) (hereafter, Linelist 3). In the case of Linelist 2 and 3, we have replaced the Li I hyper-fine structure by the same data as given in Linelist 1. All the figures shown in this work are based on the analysis using Linelist 2.

2.3. Spectral synthesis

A grid of lithium synthetic spectra has been computed for each 1D LHD and 3D CO5BOLD model atmosphere of our grid using the spectrum synthesis code Linfor3D (Steffen et al. 2015). In the 3D case, the Li I 670.8 nm line profiles were computed taking into account NLTE departure coefficients for each of the three assumed Li abundances (A(Li)=1.5, 2.0, 2.5) and the three different ^{6}Li/^{7}Li isotopic ratios (0%, 5%, 10%). For the NLTE spectral line

formation we adopted a 17-level lithium model atom, including 34 bound-bound transitions. This model was initially developed by Cayrel et al. (2007) and afterwards further updated and used by several authors (e.g., Sbordone et al. 2010, Steffen et al. 2012, Klevas et al. 2016, Mott et al. 2017, submitted).

In the 1D case, we computed a series of LTE synthetic line profiles assuming nine Li abundance values (from 1.00 to 3.00 dex with a step of 0.25 dex), six different ^{6}Li/^{7}Li isotopic ratios (from 0% to 10% with a step of 2%), and three different values of the microturbulent velocity (V_{micro}) according to the analytic expression of Dutra-Ferreira et al. (2016) and ± 0.5 km s^{-1}. Finally, to test the dependence of our results on the line list used in the spectral synthesis, we replicated the computation of the full grids of 3D NLTE and 1D

3D NLTE $T_{\rm eff}$ = 6500 K, log g = 4.0, [Fe/H] = 0.0, A(Li) = 2.0, ^{6}Li/^{7}Li = 5 %

(a)

A(Li)   = 1.980 ± 0.003
^{6}Li/^{7}Li = 9.215 ± 0.010 %
Δv   = −0.439 ± 0.047 km/s
FWHM = 8.090 ± 0.079 km/s
clevel = 1.000229 ± 0.000044
V sini = 2.00 km/s
V mic = 1.31 km/s

3D NLTE $T_{\rm eff}$ = 5900 K, log g = 4.5, [Fe/H] = 0.0, A(Li) = 2.0, ^{6}Li/^{7}Li = 5 %

(b)

A(Li)   = 1.922 ± 0.001
^{6}Li/^{7}Li = 5.745 ± 0.003 %
Δv   = −0.224 ± 0.012 km/s
FWHM = 5.232 ± 0.031 km/s
clevel = 1.000160 ± 0.000044
V sini = 2.00 km/s
V mic = 0.98 km/s
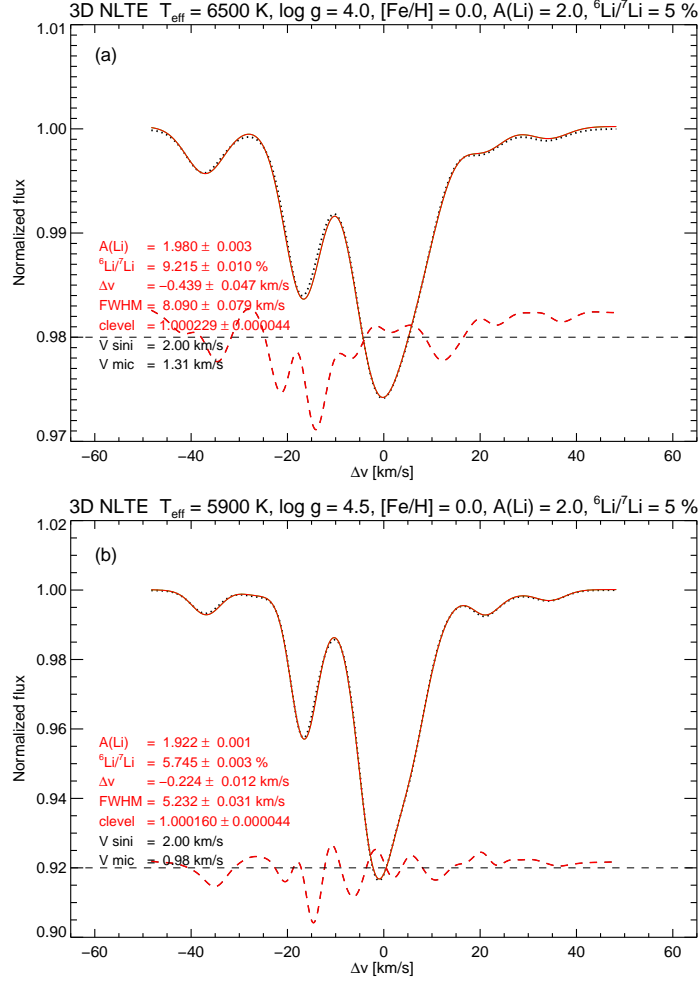
Fig. 1. The best fitting 1D LTE spectrum (red line) superimposed on the 3D NLTE spectrum (black dotted line) representing the 'observation', computed assuming [Fe/H]=0, A(Li)=2.0 and ^{6}Li/^{7}Li=5%. In panel (*a*) we adopted the model atmosphere with $T_{\rm eff}$=6500 K, log g=4.0, whereas in panel (*b*), $T_{\rm eff}$=5900 K and log g=4.5. The residuals (red dashed line) are amplified by a factor 10 and their zero-line is given as a dashed black line. The synthetic spectra are computed adopting Linelist 2 and the free fitting parameters are highlighted in red.

LTE line profiles using the sample of three different line lists mentioned above. All the synthetic spectra cover the wavelength range between 670.672 nm and 670.888 nm.

2.4. Fitting procedure and 3D NLTE corrections

For each value of A(Li) and ^{6}Li/^{7}Li of the 3D NLTE grid, we derived the corresponding 1D LTE lithium abundance and ^{6}Li/^{7}Li isotopic ratio by fitting each 3D NLTE spectrum with the grid of pre-computed 1D LTE line profiles. This is done through interpolation on the 1D LTE grid by using a least-squares fitting method MPFIT (Markwardt 2009).

Five free parameters are varied to achieve the best fit (χ^2 minimization): A(Li), ^{6}Li/^{7}Li, the continuum level (*clevel*), a global wave-
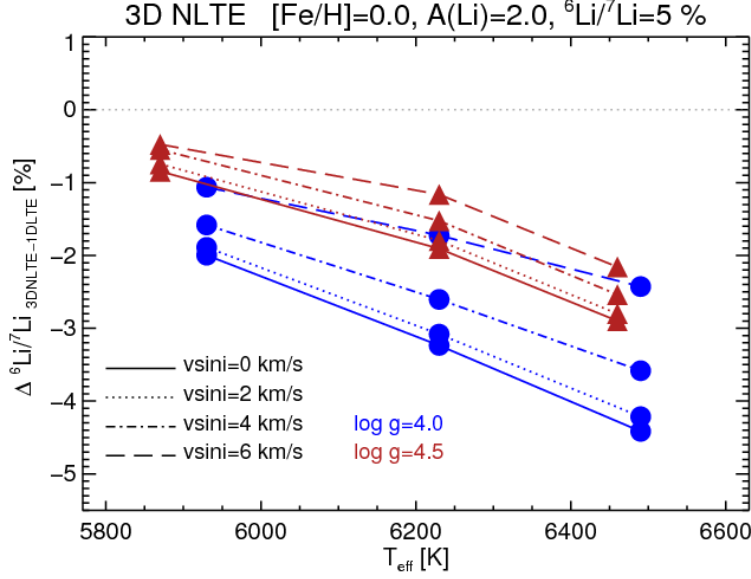
Fig. 2. ^{6}Li/^{7}Li 3D NLTE corrections versus $T_{\rm eff}$ for the 3D NLTE spectra computed assuming [Fe/H]=0, A(Li)=2, ^{6}Li/^{7}Li=5% and Linelist 2. The blue circles and the red triangles correspond to $\log g$=4 and $\log g$=4.5, respectively. The computed 3D NLTE corrections for different $v \sin i$ values are connected with lines of different styles.

length shift (Δv), and the FWHM of the Gaussian line broadening. In the 1D case, the Gaussian broadening accounts also for the macroturbulence parameter ($V_{\rm macro}$).

To investigate the possible dependence of our results on the rotational broadening, we applied an identical rotational broadening to the 3D and 1D spectra, ranging from $v \sin i = 0$ to $6 \,{\rm kms}^{-1}$ with a step of $2\,{\rm km\,s}^{-1}$. For the lithium isotopic ratio we define the 3D NLTE correction ($\Delta^6 Li/^7 Li_{\rm 3DNLTE-1DLTE}$) as the difference between the ^{6}Li/^{7}Li value assumed in the 3D NLTE synthesis and the ^{6}Li/^{7}Li value obtained from the best 1D LTE fit to the 3D NLTE spectrum.

In Fig. 1a, we show the best fit to the 3D NLTE spectrum with parameters $T_{\rm eff}$=6500 K, $\log g$=4.0, [Fe/H]=0.0, A(Li)=2.0 and ^{6}Li/^{7}Li=5%. As one can see, the ^{6}Li/^{7}Li isotopic ratio obtained in 1D LTE from the best fit overestimates the 3D NLTE ^{6}Li/^{7}Li by $\sim$ 4.2%. In Fig. 1b we show the best fit to the 3D NLTE spectrum with parameters $T_{\rm eff}$=5900 K, $\log g$=4.5, [Fe/H]=0.0,

A(Li)=2.0 and ^{6}Li/^{7}Li=5%. In this case, the ^{6}Li/^{7}Li isotopic ratio 3D NLTE correction is relatively small ($\sim$ 0.7%). Fig. 2 shows the 3D NLTE corrections for [Fe/H]=0, A(Li)=2 and ^{6}Li/^{7}Li=5%.

2.5. Analytical expression

To be able to compute the 3D NLTE ^{6}Li/^{7}Li isotopic ratio correction as a function of $T_{\rm eff}$, $\log g$ and $v \sin i$ of any target star, we derived an analytical expression, separately for each of the four metallicities. For a given [Fe/H], the formula consists of 18 numerical coefficients. As an example, we present as equation (Eq. 1) the expression we obtained for the case [Fe/H]=0:

$$\Delta^6 Li/^7 Li_{\rm 3DNLTE-1DLTE} = \sum_{i,j,k} c_{ijk} x^i y^j z^k, \quad (1)$$

where $x=(T_{\rm eff}\text{-}T_{\rm eff}^*)/T_{\rm eff}^*$, $y=\log g\text{-}\log g^*$, $z=v \sin i/{\rm km\,s}^{-1}$, i=0..2, j=0..1, k=0..2. We have chosen $T_{\rm eff}^*$=5900 K and $\log g^*$=4.0. The
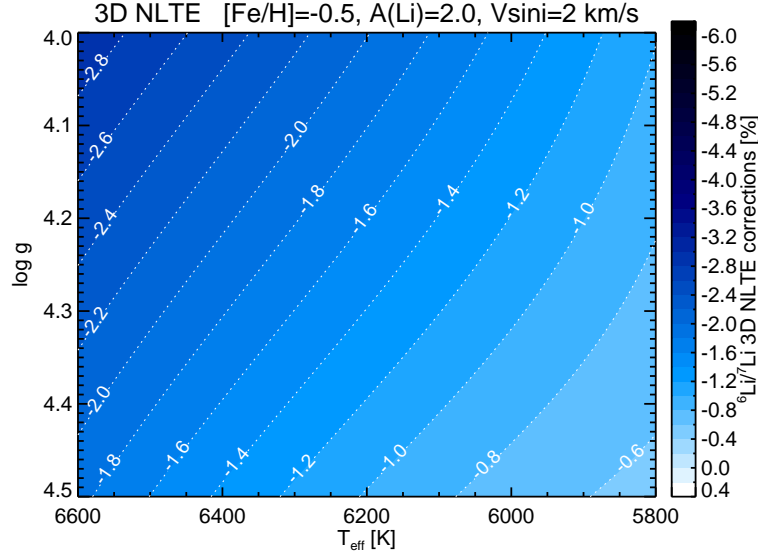
Fig. 3. Contours of ^{6}Li/^{7}Li 3D NLTE correction ($\Delta^6Li/^7Li_{\text{3DNLTE-1DLTE}}$) in the T_{eff} – $\log g$ plane for [Fe/H]=0, $v \sin i$=2 km s^{-1} and A(Li)=2, according to the analytical expression described in Section 2.5.

numerical coefficients c_{ijk} for [Fe/H]=0 are given in Table 2.

Table 2. Numerical coefficients in Eq. (1) for metallicity [Fe/H]=0 and Linelist 2.

Coeff.	Value	Coeff.	Value
c_{000}	-1.880	c_{111}	-0.632
c_{010}	1.919	c_{102}	0.424
c_{001}	0.004	c_{112}	-0.035
c_{011}	0.133	c_{200}	-25.954
c_{002}	0.024	c_{210}	-110.507
c_{012}	-0.046	c_{201}	3.062
c_{100}	-22.712	c_{211}	2.171
c_{110}	19.113	c_{202}	-0.637
c_{101}	-0.630	c_{212}	-3.469

To visualize straightforwardly the resulting 3D NLTE corrections generated with this tool, a contour plot of $\Delta^6Li/^7Li_{\text{3DNLTE-1DLTE}}$ in the T_{eff} – $\log g$ plane is presented in Fig. 3 for [Fe/H]=0 and $v \sin i$=2 km s^{-1} (A(Li)=2.0).

3. Results and discussion

We have computed ^{6}Li/^{7}Li 3D NLTE corrections for a grid of 3D NLTE spectra synthesized for combinations of four different [Fe/H], three different T_{eff}, two $\log g$, three A(Li), three ^{6}Li/^{7}Li and three different microturbulence parameters V_{micro} (see Sect. 2). Four different $v \sin i$ values of rotational broadening were applied to the spectra. All the corrections have been computed for Linelist 1, 2, and 3. In total there are 2592 ^{6}Li/^{7}Li 3D$_{\text{NLTE}}$ corrections for each list of atomic and molecular blend lines.

The ^{6}Li/^{7}Li 3D NLTE corrections show a systematic dependence on the [Fe/H], T_{eff}, $\log g$ and $v \sin i$. For given [Fe/H], they become larger with higher T_{eff}, lower $\log g$, and lower $v \sin i$. The corrections are very similar for different ^{6}Li/^{7}Li and A(Li) values of 3D NLTE spectra and for different V_{micro} values adopted for 1D synthesis. We take ^{6}Li/^{7}Li=5%, A(Li)=2 and the central value of V_{micro} as representative values.

The 3D NLTE correction of ^{6}Li/^{7}Li turned out to be very similar and almost independent of the list of the atomic and molecular data

used for spectral synthesis, which strengthens the reliability of our results.

For each metallicity, we have derived an analytical expression which allows to compute the ^{6}Li/^{7}Li 3D NLTE correction as a function of T_{eff}, log g and $v \sin i$ (see Section 2.5).

4. Conclusions

The ^{6}Li/^{7}Li isotopic ratios derived by fitting each 3D NLTE spectrum with the grid of 1D LTE line profiles are found to be always larger than the 3D NLTE values, differences ranging between 0 and 5%. This implies that a 1D LTE spectral analysis leads to an overestimation of the ^{6}Li/^{7}Li iostopic ratio by up to 5% in solar-type stars having stellar parameters within our grid. On the other hand, the 3D non-LTE corrections for the lithium abundance A(Li) are found to range between -0.01 and 0.12 dex (Harutyunyan et al., in prep.). Our analytical expressions for the 3D NLTE corrections of A(Li) and the ^{6}Li/^{7}Li ratio for solar-type stars allow to account for 3D NLTE effects without the need of a direct access to these 3D NLTE computations. This is particularly important when a large sample of stars needs to be analyzed in terms of lithium abundance and isotopic ratio, since 3D NLTE analysis for even a single target is computationally demanding and time-consuming. The analysis of the observed spectra can be carried out at first by using standard 1D LTE spectrum synthesis. Afterwards, the 1D results can be corrected for 3D non-LTE effects by applying the 3D NLTE corrections computed for the desired set of stellar parameters by means of the expressions presented in this work and in a more detailed forthcoming publication. This approach has the great advantage of directly using the results of complicated NLTE line profile synthesis with 3-dimensional model atmospheres, by-passing the actual synthesis process that would take much more time and computational resources.

The final purpose of this work is to analyze high resolution and high signal-to-noise spectra of a large sample of solar-type stars with and without giant planets. In case of any pos-

itive detection of the fragile ^{6}Li isotope in the atmosphere of our target stars, we aim to investigate its possible source (e.g., planetary material accretion, stellar flares) by looking for correlations between the derived lithium content and the presence of a planetary system and/or the level of stellar activity.

References

Caffau, E., Ludwig, H.-G., Steffen, M., et al. 2008, A&A, 488,1031

Cayrel, R., Steffen, M., Chand, H., et al. 2007, A&A, 473, L37

Delgado Mena, E., Israelian, G., González Hernández, J. I., et al. 2014, A&A, 562, A92

Dutra-Ferreira, L., Pasquini, L., Smiljanic, R., et al. 2016, A&A, 585, A75

Freytag, B., Steffen M. & Dorch, B. 2002, Astro. Nachr., 323, 213

Freytag, B., Steffen, M., Ludwig, H.-G., et al. 2012, J. Comp. Phys., 231, 919

Ghezzi, L., Cunha, K., Smith, V. V., et al. 2009, ApJ, 698, 451

Israelian, G., Santos, N. C., Mayor, M., et al. 2001, Nature, 411, 163

Klevas, J., Kučinskas, A., Steffen, M., et al. 2016, A&A, 586, A156

Kurucz, R.L. 1995, ApJ, 452, 102

Ludwig, H.-G., Caffau, E., Steffen M., et al. 2009, MmSAI, 80, 711

Markwardt, C.B. 2009, in Astronomical Data Analysis Software and Systems XVIII, ed. D. A. Bohlender, D. Durand, & P. Dowler (ASP, San Francisco), ASP Conf. Ser., 411, 251

Meléndez, J., Bergemann, M., Cohen, J. G., et al. 2012, A&A, 543, A29

Montes, D. & Ramsey, L. W. 1998, A&A, 340, L5

Mott, A., Steffen, M., Caffau, E., et al. 2017, A&A, submitted

Pinsonneault, M. 1997, ARA&A, 35, 557

Sbordone, L., Bonifacio, P., Caffau, E., et al. 2010, A&A, 522, A26

Steffen, M., Cayrel, R., Caffau, E., et al. 2012, MSAIS, 22, 152

Steffen, M., Prakapavičius, D., Caffau, E., et al. 2015, A&A, 583, A57